RSC Sustainability

ROYAL SOCIETY OF CHEMISTRY

PAPER

View Article Online
View Journal | View Issue

Cite this: *RSC Sustainability*, 2026, **4**, 803

Divergent binding modes direct functional modulation: toward next-generation ionic liquids for enzyme stabilization and biocatalysis

Swapan Patra,[a] Dharmendra Singh *[b] and Nilanjan Dey *[a]

Received 19th September 2025
Accepted 26th December 2025

DOI: 10.1039/d5su00755k

rsc.li/rscsus

Stabilizing proteolytic enzymes such as chymotrypsin (CHT) remains a major challenge due to their susceptibility to denaturation and loss of activity under non-physiological conditions. Herein, we demonstrate the use of triazolium-appended zwitterionic ionic liquids (ZILs) as efficient stabilizing agents that not only preserve but also modulate the functional properties of CHT. Spectroscopic and kinetic studies reveal distinct structure–function effects dictated by alkyl substituents. IL1, with a linear substituent, binds through electrostatic and hydrogen-bonding interactions, inducing ~3.2-fold fluorescence quenching while preserving the secondary structure. Importantly, the CHT–IL1 composite retained and even marginally enhanced catalytic activity toward a pyrenylated tyrosine substrate, underscoring the creation of a favorable microenvironment for turnover. In contrast, IL3, bearing a branched alkyl chain, inserted into hydrophobic protein pockets and stabilized a long-lived exciplex-type charge-transfer emission at 405 nm (lifetime extended from 7.8 to 13.5 ns). Docking simulations corroborated these findings, showing that IL1 stabilized CHT *via* hydrogen-bond/electrostatic contacts (−6.7 kcal mol^{-1}) whereas IL3 formed an extended hydrophobic–aromatic network with stronger binding (−7.9 kcal mol^{-1}). These results establish how structural variations in ZILs dictate protein interactions, offering valuable strategies for enzyme stabilization and functional modulation in biocatalysis.

Sustainability spotlight

This work demonstrates a sustainable strategy to enhance enzyme robustness using zwitterionic ionic liquids (ZILs). ZIL conjugation markedly extends chymotrypsin lifetime under thermal, ionic, and solvent stress, reducing enzyme consumption, waste generation, and operational costs. Molecular tunability *via* alkyl substituents enables distinct binding modes, ranging from electrostatic/hydrogen bonding to hydrophobic insertion, allowing rational, enzyme-specific stabilization without resource-intensive trial-and-error. Unlike conventional immobilization, ZILs form reversible, non-covalent complexes that preserve the protein structure and activity while avoiding harsh additives. Notably, catalytic activity is retained or marginally enhanced, improving process throughput across multiple cycles. The recyclability, low toxicity, and compatibility with aqueous/low-organic media position ZIL–enzyme composites as promising platforms for green biocatalysis, circular manufacturing, and environmental biotechnology.

Introduction

Stabilizing chymotrypsin (CHT), like many proteolytic enzymes, is challenging because of its inherent susceptibility to denaturation, autolysis, and activity loss under non-physiological conditions such as elevated temperature, extreme pH, or in the presence of organic solvents.[1] The tertiary and quaternary structures of the protein (enzyme) are maintained by a delicate network of hydrogen bonds, hydrophobic interactions, and disulfide linkages, which can be disrupted by minor environmental changes, leading to loss of catalytic activity. For instance, native CHT in aqueous buffer can lose over 50% of its activity within 2–4 hours at 45 °C, and its half-life in organic solvent systems is often less than 1 hour.[2] Stabilization strategies, such as ionic liquid (IL) conjugation, immobilization, or polymer encapsulation, are crucial as they can increase the half-life of the enzymes by several fold.[3] Such stability improvements not only extend the functional lifespan of the enzyme but also enable its application under harsher industrial, biomedical, and environmental conditions, where operational efficiency and cost-effectiveness are directly tied to enzyme durability.

Compared to conventional stabilization strategies such as immobilization on solid supports or polymer encapsulation, ionic liquid (IL) conjugation offers a more versatile and efficient approach for preserving the protein structure and activity.[4] Immobilization often results in mass transfer limitations and restricted conformational flexibility, leading to partial loss of activity (typically 10–30% reduction compared to that of the

[a]*Department of Chemistry, Birla Institute of Technology and Science Pilani, Hyderabad, India. E-mail: nilanjan@hyderabad.bits-pilani.ac.in*

[b]*Department of Applied Science & Humanities, Institute of Engineering & Technology, Dr Ram Manohar Lohia Avadh University, Ayodhya, U. P. 224001, India*

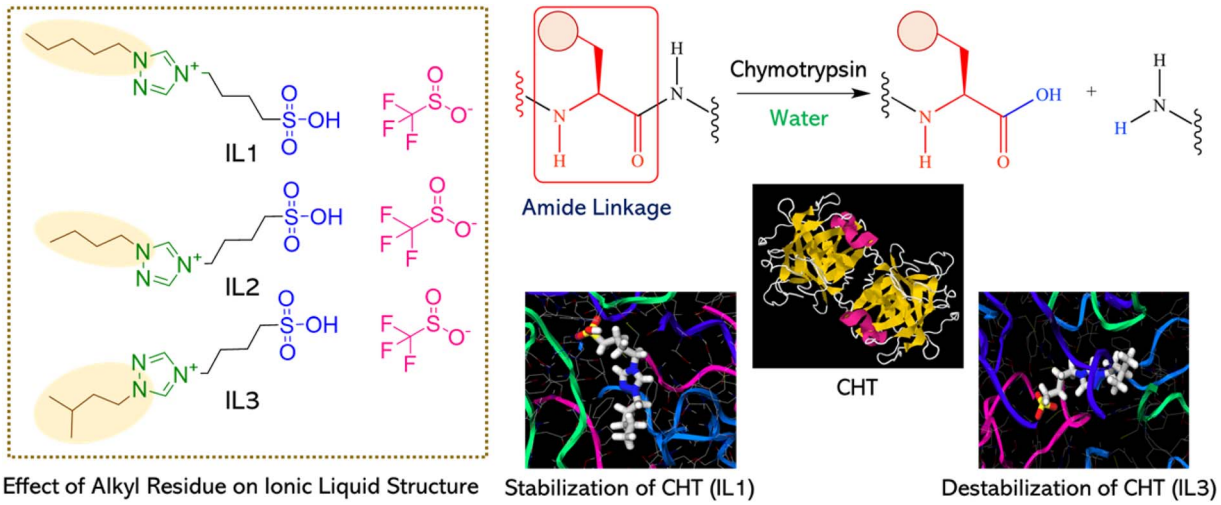

Fig. 1 Schematic diagram showing molecular structures of zwitterionic liquids involved in the present study. Also, enzymatic hydrolysis of the amide linkage by chymotrypsin (CHT).

native enzyme), while polymer encapsulation can induce diffusional barriers and heterogeneous microenvironments, slowing catalytic rates by up to 40%. In contrast, IL conjugation can provide a molecularly uniform, hydrophilic–hydrophobic balanced microenvironment that shields proteins from denaturation while maintaining high substrate accessibility.[5] For example, studies have shown that IL-protein conjugates retain >90% of their initial activity even after 30 days at 50 °C, whereas immobilized enzymes often drop below 60% under similar conditions. Moreover, IL conjugation can enhance thermal stability by increasing the melting temperature (T_m) of the protein by 5–12 °C and reducing aggregation rates by over 70%, outperforming polymer-based systems.[6] These improvements are attributed to the ability of ILs to form stabilizing ionic and hydrogen-bond interactions with surface residues, preserving the native-like hydration shell of the protein while minimizing conformational fluctuations essential for catalytic turnover.[7]

Interestingly, zwitterionic ionic liquids (ZILs) offer a superior platform for stabilizing proteins (enzymes) compared to conventional cationic or anionic ILs due to their balanced charge distribution, which minimizes electrostatic perturbation of the native conformation of proteins.[8] Unlike purely cationic ILs that may excessively interact with acidic residues or purely anionic ILs that may bind too strongly to basic residues, both of which can induce partial unfolding, ZILs possess a near-neutral net charge, reducing structural stress.[9] This charge neutrality, combined with strong hydration shell formation, can enhance retention of catalytic activity.[10] Studies have suggested that ZIL-treated enzymes can retain >90% activity after 10 days at 45 °C, compared to ~60% in cationic ILs and <40% in anionic ILs under identical conditions.[11] Additionally, ZILs can preserve the secondary structure more effectively, with far-UV CD spectra indicating <5% α-helix loss over a week, whereas cationic ILs often lead to >15% loss. Their tunable polarity also allows selective stabilization of hydrophobic pockets and prevention of aggregation, leading to ~2–3× higher residual activity after repeated thermal cycles compared to other IL types.[12]

Considering these, herein, we have studied interaction of three different triazolium appended ZILs (IL1–IL3) with chymotrypsin at pH 6.5 in buffered medium. Spectroscopic studies indicated that the nature of the alkyl substituent on the triazolium residue could dictate the contribution of different non-covalent interactions, thereby influencing its stability and catalytic activity. The IL3 with a branched alkyl chain resided in a more hydrophobic pocket of the protein, facilitating charge transfer interaction between the triazolium ion and aromatic side chains of the amino acids. In contrast, IL1 could be engaged more in hydrogen bonding and/or charge-pairing kind of interactions, which exposed the aromatic amino acids to a more polar, solvent-accessible environment. Along with investigating the stability, we also explored the catalytic activity of the CHT–IL composite in buffered medium. When a pyrene-based fluorogenic probe with tyrosine as the amino acid residue (PYR–TYR) was considered as the substrate, we observed a slight improvement in the rate of hydrolysis. This is indeed an important observation, as unlike most of the cases, herein we didn't lose the catalytic activity of CHT (rather improved marginally) at the expense of its superior stability (Fig. 1).

Results and discussion

Spectroscopic investigation with ILs

The UV-visible spectrum of chymotrypsin (CHT) in aqueous medium displayed a broad absorption band with a maximum centered at ~278 nm, arising from the π–π* electronic transitions of its aromatic amino acids, primarily tryptophan and tyrosine.[13] Upon titration with IL1, a marked hypochromic effect was observed at the 280 nm band along with a concomitant increase in absorbance near 258 nm (Fig. 2a). The hypochromic effect at 280 nm suggested a reduction in the transition probability of the aromatic chromophores, which might occur due to cation–π interactions with the triazolium headgroup, leading to partial stacking, restricted electronic delocalization, or changes in local polarity.[14] The new absorption band at 258 nm might be

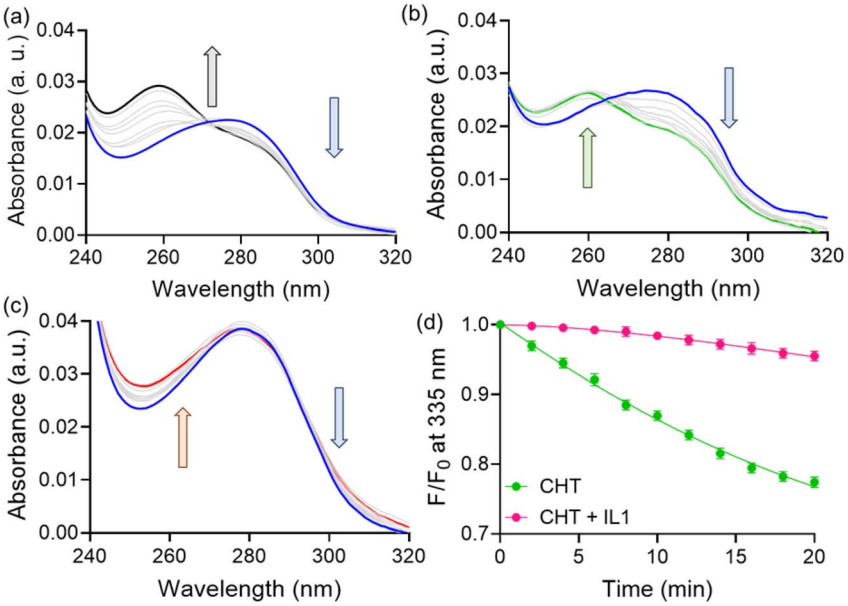

Fig. 2 UV-visible titration curves of CHT (0.1 mg mL^{-1}) with (a) IL1 (b) IL2 and (c) IL3 (0–220 μM) at pH 6.5 in buffered medium. (d) Changes in the fluorescence intensity of CHT (0.1 mg mL^{-1}, λ_{ex} = 280 nm) with time upon addition of IL1 at pH 6.5 in buffered medium.

contributed by phenylalanine residues or a blue-shifted Trp band caused by changes in hydrogen-bonding interactions within the protein microenvironment.[15] These spectral features collectively indicate that IL1 binding induces conformational rearrangements around the aromatic residues, modifying their electronic transitions. When the titration was performed with IL2 (Fig. 2b), qualitatively similar spectral changes were observed, but with a more pronounced hypochromic shift, implying either stronger binding or a more extensive perturbation of the aromatic residue environments compared to IL1. In contrast, exposure of CHT to IL3 did not produce a hypochromic shift at 280 nm, and the 258 nm region remained largely unaffected (Fig. 2c). This absence of the expected aromatic perturbation suggests that IL3 interacts with CHT through a different mode, possibly binding to surface hydrophobic domains without significantly altering the electronic transitions of Trp/Tyr in their ground state. Such differences in the UV-visible response hint at distinct spatial orientations or binding sites for IL3 compared to IL1 and IL2.

The fluorescence spectrum of CHT in aqueous medium exhibited a dominant emission maximum at 335 nm, characteristic of tryptophan residues in a relatively non-polar

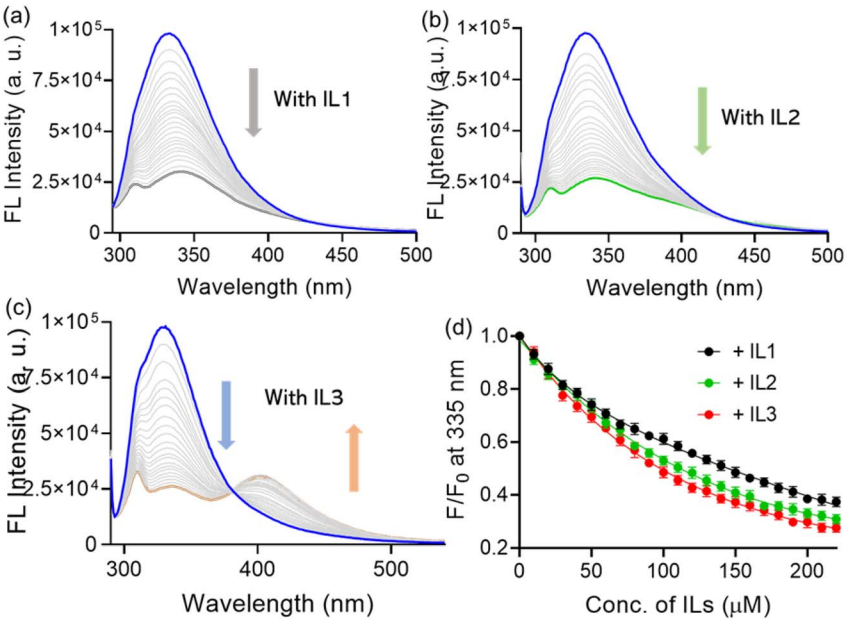

Fig. 3 Fluorescence titration curves of CHT (0.1 mg mL^{-1}, λ_{ex} = 280 nm) with (a) IL1 (b) IL2 and (c) IL3 (0–220 μM) at pH 6.5 in buffered medium. (d) Changes in the fluorescence intensity of CHT (0.1 mg mL^{-1}, λ_{ex} = 280 nm) upon addition of various ILs at pH 6.5 in buffered medium.

environment (Fig. 3a). Addition of IL1 resulted in a concentration-dependent (0–220 μM) quenching of emission intensity (~3.2-fold) with a ~10 nm red shift in λ_{max}. This bathochromic shift suggests that Trp residues become more solvent-exposed upon IL1 binding, experiencing a more polar and hydrogen-bonding-rich environment due to conformational rearrangements.[16] Fluorescence titration with IL2 (Fig. 3b) produced a similar overall quenching (~3.5-fold), but was accompanied by a small hump at ~405 nm, indicating the formation of a minor long-wavelength emissive species, likely an exciplex or excited-state charge-transfer (CT) complex.[17] Interestingly, titration with IL3 caused a ~3.7-fold decrease in the 335 nm band with the simultaneous growth of a pronounced new emission at ~405 nm (Fig. 3c). The prominent long-wavelength band is consistent with efficient excited-state CT between Trp (electron donor) and the triazolium ring (electron acceptor) of the IL.[18] The branched alkyl group in IL3, with its greater hydrophobic surface area compared to straight-chain analogues, likely promotes deeper insertion into hydrophobic protein cavities near aromatic residues. This positioning fixes the triazolium moiety in close proximity to Trp, strengthening cation–π interactions and stabilizing the CT complex, thereby enhancing its emission (Fig. 3d). The interactions of CHT with ILs were found to be a time-dependent phenomenon. To examine this, we incubated CHT with excess IL1 (0.25 mM) for 30 min, and changes in the fluorescence intensity (at 335 nm) were recorded at an interval of 2 min (Fig. 2d). The saturation in the fluorescence response was observed at ~20–22 min. This gradual, time-dependent quenching behaviour suggests that IL1 initially forms a weak encounter complex with CHT through diffusion-controlled interactions, which subsequently evolves into a more stable, ground-state association as the enzyme undergoes slower conformational rearrangements around the bound ionic liquid, consistent with a static quenching mechanism.

Effects of the microenvironment on IL binding

To gain mechanistic insight into the optical response, a series of spectroscopic studies were carried out with IL1. First, the effect of ionic strength on the fluorescence response of IL1 toward CHT was examined. In the presence of 5 M NaCl, the extent of fluorescence quenching was markedly reduced, with only ~1.25-fold quenching observed compared to the salt-free condition (Fig. 4a). This attenuation suggests that electrostatic interactions play a significant role in the IL1–CHT association. Next, fluorescence titration of CHT with IL1 was performed at an elevated temperature (50 °C) under otherwise identical conditions. At this temperature, the addition of IL1 produced only ~1.43-fold quenching of the emission intensity, approximately 2.2-fold lower than that observed during titration at 25 °C (Fig. 4b). The reduced quenching efficiency at higher temperatures is likely due to partial thermal unfolding of CHT, which disrupts the native aromatic microenvironment and may weaken specific non-covalent interactions between IL1 and the protein.[19] To further quantify the temperature-dependent interaction between IL1 and CHT, the binding constant (K_b) was determined from the modified Stern–Volmer equation. The binding constant values were obtained as 2.4×10^{-2} M^{-1} at 25 °C and 1.3×10^{-4} M^{-1} at 50 °C, respectively (Fig. S11). The sharp decline in K_b with temperature confirms that the quenching mechanism is predominantly static, as elevated temperature disrupts the ground-state IL1–CHT complex. The thermodynamic analysis based on the Van't Hoff relation yielded $\Delta H = +167$ kJ mol^{-1} and $\Delta S = +0.53$ kJ mol^{-1}

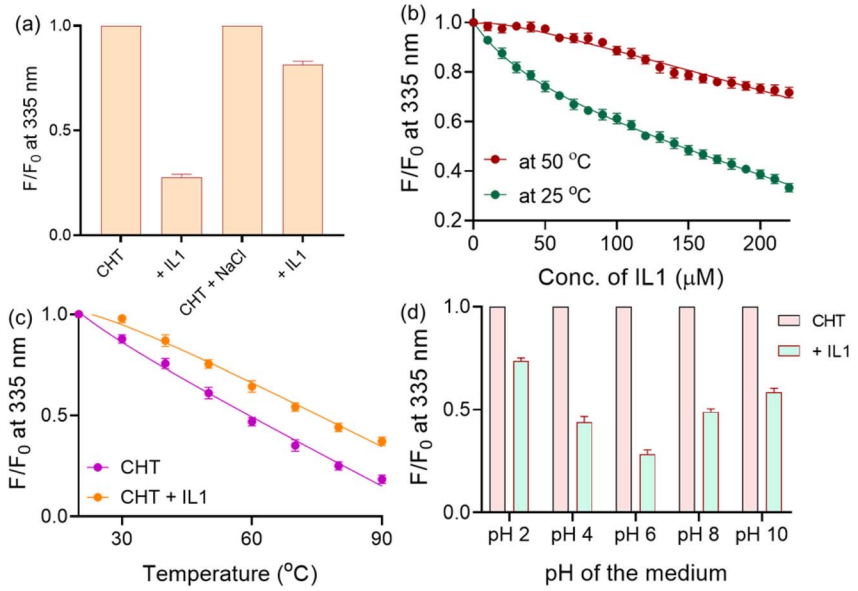

Fig. 4 (a) Changes in the FL intensity of CHT (0.1 mg mL^{-1}, $\lambda_{ex} = 280$ nm) with IL1 (220 μM) in the presence of NaCl (5 M) at pH 6.5 in buffered medium. (b) Changes in the FL intensity of CHT (0.1 mg mL^{-1}, $\lambda_{ex} = 280$ nm) with IL1 (0–220 μM) at different temperatures in buffered medium (at pH 6.5). (c) Effect of temperature on the stability of CHT (0.1 mg mL^{-1}) and CHT. IL1 composite in buffered medium (at pH 6.5). (d) Effect of pH on interaction of CHT (0.1 mg mL^{-1}, $\lambda_{ex} = 280$ nm) with IL1 (220 μM) in buffered medium (at pH 6.5).

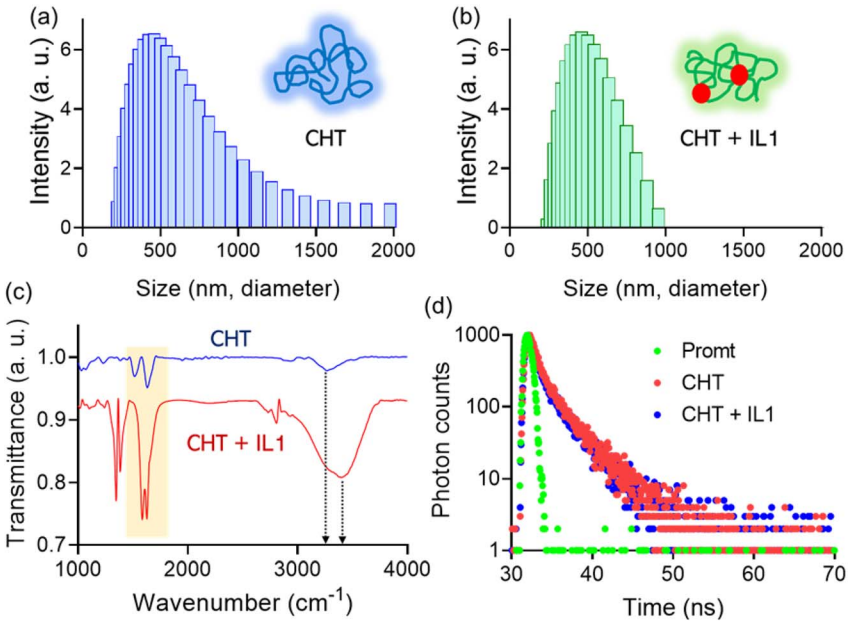

Fig. 5 Determination of the hydrodynamic diameter of CHT (0.1 mg mL^{-1}, λ_{ex} = 280 nm) in the (a) absence and (b) presence of IL1 (220 μM) at pH 6.5 in buffered medium using DLS. (c) FT-IR spectra of CHT (0.1 mg mL^{-1}) with and without IL1. (d) Fluorescence decay spectra of CHT (0.1 mg mL^{-1}, λ_{ex} = 280 nm) at 335 nm upon addition of IL1 (220 μM) at pH 6.5 in buffered medium.

K^{-1}, giving ΔG values of +9.3 kJ mol^{-1} (25 °C) and +23.3 kJ mol^{-1} (50 °C). The positive ΔH indicates an endothermic process that weakens at higher temperatures, while the large positive ΔS suggests an entropy-driven association dominated by desolvation and hydrophobic rearrangement. Overall, the IL1–CHT binding is mainly governed by electrostatic and hydrogen-bonding interactions with favourable entropy gain, consistent with a static quenching mechanism. The fact that both high ionic strength and elevated temperature diminish the quenching efficiency indicates that IL1–CHT binding is governed by electrostatically mediated, conformation-dependent interactions. Furthermore, the observed hypochromic shifts in the UV-visible spectrum and the red-shift in the fluorescence maxima upon IL1 binding suggest the formation of a ground-state complex between IL1 and CHT, consistent with a predominantly static quenching mechanism.[20]

Further, to confirm the nature of the quenching phenomenon, we recorded time-resolved fluorescence spectra of CHT in the presence of IL1 (Fig. 5d). The average excited-state lifetime of native CHT was found to be 2.1 ns (tri-exponential decay). Despite the fluorescence quenching observed in steady-state analysis, the average lifetime remained essentially unchanged upon addition of IL1. This strongly supports the formation of a non-fluorescent ground-state electrostatic complex between CHT and IL1.[21] Interestingly, when both native CHT and the CHT–IL1 complex were subjected to temperature-dependent fluorescence studies (25–90 °C), the extent of fluorescence quenching was less prominent for the complex than for the native protein (Fig. 4c). This observation suggests that IL1 binding confers partial conformational stabilization to CHT, likely by shielding key aromatic residues from solvent exposure and reducing thermally induced unfolding.

Furthermore, we examined the interaction of CHT with IL1 under different pH conditions in buffered media. For better comparison, the fluorescence intensity of free CHT at each pH was normalized to unity, and the extent of quenching upon IL1 addition was expressed as the ratio F/F_0 at 332 nm (Fig. 4d). The quenching efficiency was found to be maximum at pH 6 and decreased progressively under both acidic and alkaline conditions. This pH dependence can be explained by changes in the ionization state of key amino acid residues and the net surface charge of both CHT and IL1. At pH 6, which is close to the isoelectric point of CHT, electrostatic repulsion is minimized, enabling closer association and stronger complex formation between CHT and IL1, leading to more efficient quenching. Under acidic conditions (pH < 6), excess protonation of acidic side chains increases the net positive charge on CHT, possibly enhancing repulsion with positively charged groups of IL1 and disturbing the optimal orientation for interaction. Conversely, under alkaline conditions (pH > 6), partial unfolding or loosening of the tertiary structure of the protein may disrupt the integrity of the hydrophobic binding pocket, reducing the affinity for IL1.[22] Additionally, increased solvation of both the protein and IL at a high pH might weaken hydrophobic interactions, while enhanced conformational flexibility may reduce the stability of any transient complexes formed, thereby lowering quenching efficiency despite favorable electrostatics.[23]

Mechanistic investigation

Dynamic light scattering (DLS) analysis of native CHT revealed a dominant intensity-weighted hydrodynamic diameter of ~380 nm (PdI = 0.12), with a low-intensity tail toward larger sizes, consistent with a predominantly monomeric enzyme population and a minor fraction of transient oligomers (Fig. 5a).

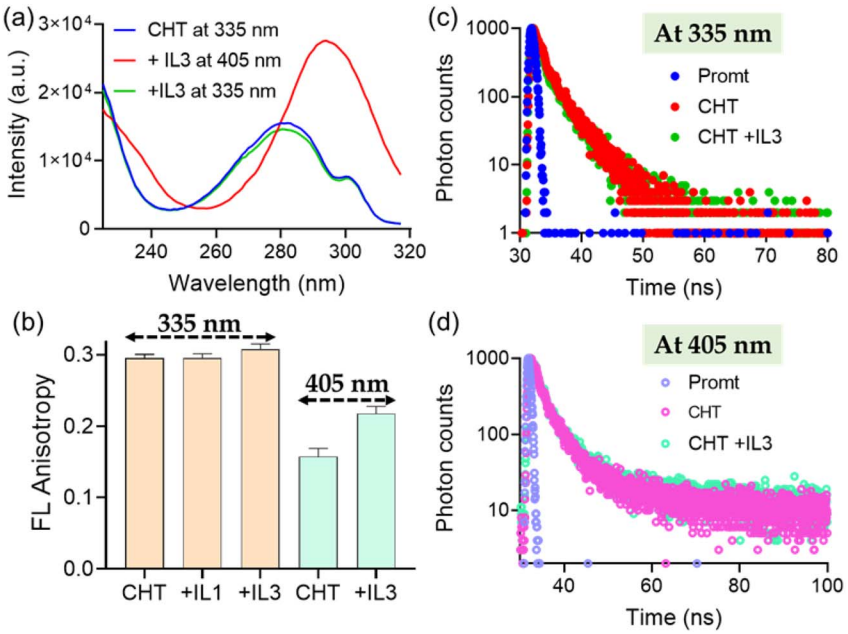

Fig. 6 (a) Fluorescence excitation spectra of CHT (0.1 mg mL^{-1}) with IL3 (220 μM) at 335 nm and 405 nm at pH 6.5 in buffered medium. (b) Fluorescence anisotropy of CHT (0.1 mg mL^{-1}) with IL1 and IL3 (220 μM) at 335 and 405 nm in buffered medium (at pH 6.5). Fluorescence decay spectra of CHT (0.1 mg mL^{-1}, λ_{ex} = 280 nm) upon addition of IL3 (220 μM) at (c) 335 and (d) 405 nm in buffered medium (at pH 6.5).

Upon addition of IL1, the principal peak shifted to ~433 nm, accompanied by an increase in the PdI to 0.34 (Fig. 5b). This shift reflects the formation of IL–protein complexes, likely arising from IL adsorption and the development of IL-rich assemblies on the enzyme surface. Mechanistically, the cationic triazolium ring of IL1 can engage in electrostatic and cation–π interactions with negatively charged and aromatic residues (*e.g.*, Trp and Tyr) on CHT, while its hydrophobic alkyl chain can insert into nonpolar surface pockets. These interactions enlarge the hydrodynamic radius and, at higher local IL concentrations, may promote weak multimerization or bridging between enzyme molecules.[24]

FT-IR spectroscopy of native CHT showed amide I and amide II bands at 1631 cm^{-1} and 1516 cm^{-1}, respectively, characteristic of a predominantly α-helical/turn-rich secondary structure (Fig. 5c). Upon incubation with IL1, the amide I band downshifted to 1625 cm^{-1}, accompanied by a noticeable change in band contour. The amide II band shifted to a higher energy region, at 1585 cm^{-1}. Such shifts point to perturbations in backbone C=O stretching and N–H bending modes, indicative of altered hydrogen-bonding patterns and a partial reorganization or loosening of the secondary structure, likely increasing the fraction of solvent-exposed peptide segments.[25] New absorption bands appeared in the fingerprint region at ~1387 cm^{-1} and ~1353 cm^{-1}, assignable to the asymmetric and symmetric stretching modes of the S=O/CF_3–SO_3^- groups, confirming adsorption of IL1 onto the protein surface. In addition, the broad –NH/–OH stretching band originally centred at ~3277 cm^{-1} became broader and shifted to a higher energy-zone (~3287 cm^{-1}), consistent with modification of the hydrogen-bonding network, possibly due to increased solvation or electrostatic interactions introduced by the IL1 anions and cations. Collectively, the DLS and FT-IR results indicate that IL1 associates with CHT through a combination of electrostatic, cation–π, and hydrophobic interactions, positioning the triazolium headgroup near aromatic residues and embedding the alkyl tail within hydrophobic patches, leading to modest increases in hydrodynamic size and minor secondary structure rearrangements, without extensive denaturation.

The origin of the new emission band at ~405 nm was probed using excitation, fluorescence anisotropy, and lifetime measurements. The excitation spectrum of native CHT monitored at 335 nm displayed the expected maximum around 280 nm, characteristic of aromatic residues, and remained essentially unchanged upon IL3 addition, indicating that the ground-state absorption of Trp/Tyr residues was not significantly perturbed (Fig. 6a). In sharp contrast, when the emission was monitored at 405 nm in the presence of IL3, a distinctly different excitation profile emerged with a maximum shifted toward 290–300 nm and significantly higher intensity. This spectral separation clearly suggests that the 405 nm band does not originate from conventional Trp fluorescence but rather from a new excited-state species. Fluorescence anisotropy measurements provided further evidence (Fig. 6b). Native CHT exhibited an anisotropy of 0.2911 at 335 nm, consistent with localized Trp emission in a rigid environment, which slightly increased to 0.3031 upon IL3 addition, reflecting reduced Trp mobility due to binding. At 405 nm, native CHT displayed a much lower anisotropy of 0.1495, indicative of depolarized emission from a flexible or delocalized excited state.[26,27] Strikingly, the anisotropy increased to 0.2108 for the CHT–IL3 system at 405 nm, suggesting stabilization of this long-wavelength emissive species within the protein matrix.[28,29] By contrast, IL1 addition caused a negligible anisotropy change

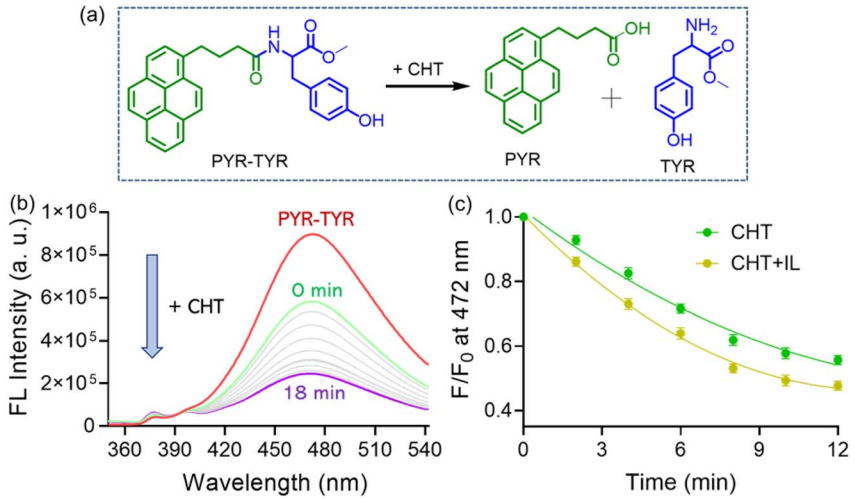

Fig. 7 (a) Schematic diagram showing enzymatic cleavage of PYR–TYR. (b) Changes in fluorescence spectra of PYR–TYR (10 mM) with time upon addition of the CHT–IL composite at pH 7.4 in buffered medium. (c) Changes in the fluorescence intensity of PYR–TYR at 472 nm upon addition of CHT (0.1 mg mL^{-1}) with IL1 (220 μM) in buffered medium (at pH 7.4).

(0.2917 at 335 nm), underscoring the unique role of IL3. Time-resolved fluorescence analysis reinforced these findings. The average lifetime of native CHT at 335 nm was 2.18 ns, typical for Trp emission, and remained nearly unchanged upon IL3 addition (2.05 ns), confirming that the intrinsic Trp excited state was not perturbed (Fig. 6c).[30] In contrast, when monitored at 405 nm, native CHT exhibited a much longer lifetime of 7.8 ns, consistent with emission from a secondary excited-state species distinct from Trp. Remarkably, the lifetime of the 405 nm band increased to 13.5 ns in the CHT–IL3 system (Fig. 6d), demonstrating that IL3 stabilizes this long-lived emissive state. Taken together, the distinct excitation profile, enhanced anisotropy, and prolonged excited-state lifetime strongly support assignment of the 405 nm band to an exciplex-type charge-transfer state formed between Trp residues (electron donor) and the triazolium moiety of IL3 (electron acceptor).[31] The branched alkyl chain of IL3 likely promotes deeper insertion into hydrophobic protein pockets, positioning the triazolium group in close proximity to Trp, enhancing donor–acceptor orbital overlap, and thereby stabilizing the CT state. This close spatial arrangement accounts for the emergence, rigidity, and long-lived nature of the prominent 405 nm emission.

Catalytic activity of the CHT–IL composite

Since the experimental evidence indicated improved stability of the CHT–IL1 composite compared to native CHT, we further investigated its effect on catalytic efficiency. For a typical experiment, we used a pyrenylated tyrosine derivative (PYR–TYR) in an aqueous medium and monitored the hydrolysis in the presence of CHT and the CHT–IL1 composite (Fig. 7a). The fluorescence spectrum of PYR–TYR displayed a broad emission band with a maximum at ~472 nm. The addition of both CHT and CHT–IL1 resulted in a time-dependent (0–18 min) quenching of fluorescence intensity (Fig. 7b). When the changes in the fluorescence intensity at the 472 nm band were plotted against the incubation time, a pseudo-first-order kinetic response was observed in both cases. The formation of the expected hydrolysis product was further confirmed by LC-MS analysis, which revealed a molecular ion corresponding to the cleaved derivative (Fig. S10). Interestingly, CHT–IL1 showed a slightly improved hydrolysis rate compared to native CHT (Fig. 7c). This enhancement could be attributed to the ability of the ionic liquid to create a more favorable microenvironment, possibly improving substrate accessibility and retaining an active conformation of the catalytic site.[32] The IL may also facilitate more efficient solubilization and orientation of the substrate, leading to faster turnover. Thus, the presence of IL1 not only stabilized the secondary structure of the protein but also contributed to improved catalytic activity. To further contextualize these results, we compared our observations with previously reported studies employing imidazolium and phosphonium-based ionic liquids (ILs) for similar proteolytic systems. Prior reports indicate that while imidazolium ILs enhance the thermal stability of α-chymotrypsin through cation–π and hydrophobic interactions, they frequently lead to partial rigidification of the catalytic domain and reduction in its activity. Similarly, phosphonium ILs have been shown to confer high thermostability but at the cost of diminished catalytic turnover. In contrast, the ZILs designed in this work provide a balanced electrostatic–hydrophobic microenvironment that preserves the secondary structure and even enhances catalytic efficiency. A detailed comparative summary of these systems is provided in Table S2 (SI).

Computational insights

Docking analysis revealed that IL1 localized near the catalytic triad region of chymotrypsin, engaging in multiple stabilizing interactions (Fig. 8a). Prominent hydrogen bonds were observed with Tyr146 (2.3 Å) and Ser195 (2.8 Å), along with an electrostatic contact with His57 (3.1 Å). Several neighboring residues contributed to the stability of this binding mode: Asp194 added polarity near the oxyanion hole, Gly214–216 provided flexible loop contacts, and

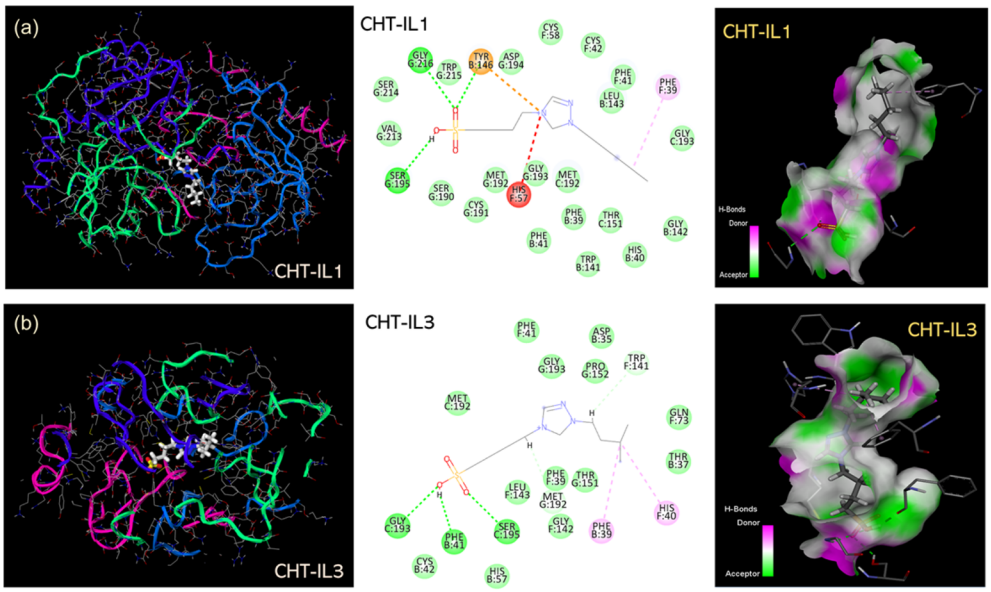

Fig. 8 (a) 3D-binding interaction between CHT and IL1, and 2D interaction of CHT with IL1, highlighting the type of bond and non-covalent interactions. (b) 3D-binding interaction between CHT and IL3, and 2D interaction of CHT with IL3, highlighting the type of bond and non-covalent interactions.

Leu143 and Phe41 flanked the hydrophobic face of the alkyl chain. Additionally, Met192 and Gly193 formed a shallow groove, partially embedding the triazolium group, while Trp215 stabilized the IL *via* cation–π interaction (~3.4 Å), consistent with the observed ~3.2-fold quenching and a 10 nm red shift in Trp fluorescence.[33] The overall binding affinity was −6.7 kcal mol^{-1}, reflecting moderate but specific stabilization. Importantly, this interaction network preserved the protein's secondary structure and enhanced catalytic efficiency: hydrolysis of the pyrenylated tyrosine substrate exhibited an apparent rate constant of 0.041 min^{-1} compared to 0.032 min^{-1} for native CHT (~28% improvement), indicating that IL1 provides an electrostatically balanced environment that retains and even enhances enzymatic function.

In contrast, IL3 inserted more deeply into hydrophobic cavities, forming a broader network of predominantly aromatic and nonpolar interactions (Fig. 8b). Strong hydrophobic and π–π stacking contacts were observed with Phe39 (3.6 Å), Phe41 (3.8 Å), and Phe142, while Trp141 at ~3.5 Å acted as an electron donor to the triazolium headgroup, directly contributing to exciplex stabilization. The branched alkyl substituent was anchored by Leu143 and Met192, while Thr151 and Pro152 added steric support that locked the ligand into place. Peripheral residues such as Asp35 and His40 modulated local polarity, whereas Gly193 (2.9 Å) and Ser195 (3.1 Å) provided weak hydrogen-bonding contacts. This extended hydrophobic–aromatic cage accounted for the stronger binding affinity of −7.9 kcal mol^{-1} and the emergence of a distinct long-wavelength emissive species at 405 nm. Fluorescence anisotropy increased from 0.1495 (native CHT) to 0.2108 (CHT–IL3) at 405 nm, and the excited-state lifetime was prolonged from 7.8 ns to 13.5 ns, confirming stabilization of a long-lived charge-transfer state between Trp and the triazolium ring.[34] Thus, while IL1 promotes catalytic stability through electrostatic and hydrogen-bonding interactions, IL3 directs its effect toward stabilization of an exciplex-type CT state by embedding into an aromatic-rich hydrophobic pocket, illustrating how structural variation of the alkyl substituent drives divergent functional modulation of chymotrypsin.

Conclusion

This work demonstrates how triazolium-appended zwitterionic ionic liquids (ZILs) stabilize and modulate the properties of chymotrypsin (CHT), with their effects strongly dependent on the nature of the alkyl substituents. IL1 primarily engaged through electrostatic and hydrogen-bonding interactions, evident from a ~3.2-fold quenching of Trp emission at 332 nm accompanied by a ~10 nm red shift and hypochromic perturbations in UV-visible spectra. The quenching efficiency decreased at high ionic strength (only ~1.25-fold quenching in 5 M NaCl) and elevated temperature (1.43-fold at 50 °C), confirming the electrostatic and conformation-dependent nature of IL1 binding. DLS and FT-IR analyses further indicated modest structural reorganization without extensive denaturation. Notably, the CHT–IL1 composite retained enzymatic function and showed a slight improvement in catalytic efficiency, as reflected in a faster pseudo-first-order hydrolysis of a pyrenylated tyrosine derivative compared to native CHT, highlighting the ability of IL1 to create a more favorable microenvironment for substrate accessibility and turnover. Docking simulations supported these findings, showing that IL1 stabilized CHT *via* hydrogen bonds with Tyr146 (2.3 Å) and Ser195 (2.8 Å), and electrostatic contact with His57 (3.1 Å), along with additional support from nearby residues such as Asp194, Gly214–216, and Trp215, resulting in a binding affinity of −6.7 kcal mol^{-1}.

In contrast, IL3 exhibited a strikingly different behavior. While the ground-state absorption of aromatic residues was

unaffected, fluorescence studies revealed a ~3.7-fold quenching at 332 nm accompanied by a pronounced new emission at ~405 nm. Excitation spectra, anisotropy, and lifetime data established this as an exciplex-type charge-transfer (CT) state between Trp residues and the triazolium ring of IL3. Anisotropy at 405 nm increased from 0.1495 (native CHT) to 0.2108 with IL3, while the excited-state lifetime was prolonged from 7.8 ns to 13.5 ns, confirming stabilization of a long-lived CT state, facilitated by deeper insertion of the branched alkyl chain into hydrophobic pockets. Docking revealed that IL3 was anchored predominantly by hydrophobic and aromatic interactions with Phe39, Phe41, Phe142, Trp141, Leu143, and Met192, with weaker hydrogen bonds from Gly193 (2.9 Å) and Ser195 (3.1 Å), yielding a stronger binding affinity of −7.9 kcal mol^{-1}. Overall, IL1 confers electrostatic stabilization while preserving and modestly enhancing catalytic activity, whereas IL3 stabilizes a unique CT emissive state through hydrophobic insertion. These insights, combining spectroscopic, kinetic, and docking evidence, reveal a clear structure–function relationship in IL–protein interactions, guiding the rational design of ILs for simultaneous enzyme stabilization and functional modulation.

Author contributions

Swapan Patra: writing – original draft, visualization, validation, methodology, investigation. Dharmendra Singh: methodology, writing – original draft, visualization, validation, supervision, software. Nilanjan Dey: writing – review & editing, supervision, resources, project administration, investigation, funding acquisition, formal analysis, conceptualization.

Conflicts of interest

There are no conflicts to declare.

Data availability

Data will be made available on request.

Supplementary information (SI): synthetic routes for the ionic liquids, along with their corresponding ^{1}H NMR and ^{13}C NMR spectral data. See DOI: https://doi.org/10.1039/d5su00755k.

Acknowledgements

ND thanks VB Ceramic Consultants for financial support and a fellowship to SP. The authors thank the BITS Pilani Hyderabad campus for technical support and DS thanks Dr. Ram Manohar Lohia Avadh University for both technical and financial support.

References

1 S. Timr and F. Sterpone, Stabilizing or Destabilizing: Simulations of Chymotrypsin Inhibitor 2 under Crowding Reveal Existence of a Crossover Temperature, *J. Phys. Chem. Lett.*, 2021, **12**(6), 1741–1746.
2 C. Bahamondes, A. Illanes, L. Wilson and R. Conejeros, Mathematical Determination of Kinetic Parameters for Assessing the Effect of the Organic Solvent on the Selectivity of Peptide Synthesis with Immobilized α-Chymotrypsin, *J. Biosci. Bioeng.*, 2017, **124**(6), 618–622.
3 M. Bisht and P. Venkatesu, Influence of Cholinium-Based Ionic Liquids on the Structural Stability and Activity of α-Chymotrypsin, *New J. Chem.*, 2017, **41**(22), 13902–13911.
4 S. Patra, P. Singh, D. Singh and N. Dey, Conformational Stability of α-Lactalbumin and Lysozyme in Ammonium-Based Ionic Liquids: A Comprehensive Insight into Structure–Activity Relationship, *Ind. Eng. Chem. Res.*, 2025, **64**(5), 2543–2552.
5 P. Bharmoria, A. A. Tietze, D. Mondal, T. S. Kang, A. Kumar and M. G. Freire, Do Ionic Liquids Exhibit the Required Characteristics To Dissolve, Extract, Stabilize, and Purify Proteins? Past–Present–Future Assessment, *Chem. Rev.*, 2024, **124**(6), 3037–3084.
6 M. Bisht, D. Mondal, M. M. Pereira, M. G. Freire, P. Venkatesu and J. A. P. Coutinho, Long-Term Protein Packaging in Cholinium-Based Ionic Liquids: Improved Catalytic Activity and Enhanced Stability of Cytochrome c against Multiple Stresses, *Green Chem.*, 2017, **19**(20), 4900–4911.
7 P. Bharadwaj, A. Barua, M. Bisht, D. K. Sarkar, S. Biswas, G. Franklin and D. Mondal, Understanding the Effect of Ionic Liquid–Mediated Solvent Engineering on the Kinetics and Thermodynamic Stability of Phenylalanine Ammonia-Lyase, *J. Phys. Chem. B*, 2024, **128**(38), 9102–9110.
8 D. Chand, M. Wilk-Kozubek, V. Smetana and A.-V. Mudring, Alternative to the Popular Imidazolium Ionic Liquids: 1,2,4-Triazolium Ionic Liquids with Enhanced Thermal and Chemical Stability, *ACS Sustain. Chem. Eng.*, 2019, **7**(19), 15995–16006.
9 S. Selvam, S. Cheriyathennatt, P. Ratheesh, A. Ashraf, A. Satheesh and E. Kandasamy, Photophysical Study on Synthesized Triazolium Ionic Liquids and Their Stabilizing Effect on Native State of Serum Albumin, *J. Mol. Liq.*, 2024, **409**, 125463.
10 F. Philippi and T. Welton, Targeted Modifications in Ionic Liquids—From Understanding to Design, *Phys. Chem. Chem. Phys.*, 2021, **23**(12), 6993–7021.
11 Y. Gu, L. Shi, X. Cheng, F. Lu and L. Zheng, Aggregation Behavior of 1-Dodecyl-3-methylimidazolium Bromide in Aqueous Solution: Effect of Ionic Liquids with Aromatic Anions, *Langmuir*, 2013, **29**(21), 6213–6220.
12 P. Alam, K. Siddiqi, S. K. Chaturvedi and R. H. Khan, Protein Aggregation: From Background to Inhibition Strategies, *Int. J. Biol. Macromol.*, 2017, **103**, 208–219.
13 R. S. Fernandes, A. Gangopadhyay and N. Dey, Shedding Light on Protein Aggregates by Bisindolyl-Based Fluorogenic Probes: Unveiling Mechanistic Pathways and Real-Time Tracking of Protein Aggregation, *Biomacromolecules*, 2025, **26**(3), 1461–1475.
14 S. Patra and N. Dey, Unravelling the Optical Properties and Self-Assembly Behavior of Ciprofloxacin in Ionic Liquid Environments: Probing the Role of Cationic Residues and Counter Anions, *Dalton Trans.*, 2025, **54**(13), 5502–5510.

15 J. Raw, L. R. Franco, L. F. d. C. Rodrigues and L. R. S. Barbosa, Unveiling the Three-Step Model for the Interaction of Imidazolium-Based Ionic Liquids on Albumin, *ACS Omega*, 2023, **8**(41), 38101–38110.
16 A. Mukhopadhayay, D. Singh and K. P. Sharma, Neat Ionic Liquid and α-Chymotrypsin–Polymer Surfactant Conjugate-Based Biocatalytic Solvent, *Biomacromolecules*, 2019, **21**(2), 867–877.
17 A. Yadav, S. Trivedi, V. Haridas, J. B. Essner, G. A. Baker and S. Pandey, Effect of Ionic Liquid on the Fluorescence of an Intramolecular Exciplex Forming Probe, *Photochem. Photobiol. Sci.*, 2020, **19**(2), 251–260.
18 A. Singh, S. Sharma, N. Kaur and N. Singh, Self-Assembly of Imidazolium/Benzimidazolium Cationic Receptors: Their Environmental and Biological Applications, *New J. Chem.*, 2020, **44**(44), 19360–19375.
19 L. Mirdha and H. Chakraborty, Fluorescence Quenching by Ionic Liquid as a Potent Tool To Study Protein Unfolding Intermediates, *J. Mol. Liq.*, 2020, **312**, 113408.
20 S. Patil, S. Pise and N. Dey, Tuneable Charge-Transfer Probes for Environmental Monitoring: Phthalimide-Linked Pyrene-Dione Probes for Ratiometric Sensing of Cu^{2+}, *J. Mol. Struct.*, 2025, **1337**, 142103.
21 N. Dey, A Pyrene-Based Ratiometric Probe for Nanomolar Level Detection of Glyphosate in Food and Environmental Samples and Its Application for Live-Cell Imaging, *New J. Chem.*, 2022, **46**(17), 8105–8111.
22 X. Zhao, T. Xing, X. Xu and G. Zhou, Influence of Extreme Alkaline pH Induced Unfolding and Aggregation on PSE-like Chicken Protein Edible Film Formation, *Food Chem.*, 2020, **319**, 126574.
23 J. Hladilkova, T. H. Callisen and M. Lund, Lateral Protein–Protein Interactions at Hydrophobic and Charged Surfaces as a Function of pH and Salt Concentration, *J. Phys. Chem. B*, 2016, **120**(13), 3303–3310.
24 E. Sedghamiz and M. Moosavi, Tricationic Ionic Liquids: Structural and Dynamical Properties *via* Molecular Dynamics Simulations, *J. Phys. Chem. B*, 2017, **121**(8), 1877–1892.
25 N. N. Brandt, A. A. Mankova and A. Y. Chikishev, IR Spectroscopy of Structural Changes of α-Chymotrypsin Related to the Changes of Function in Organic Solvents, *Mosc. Univ. Phys. Bull.*, 2011, **66**(3), 282–285.
26 S. Mondal and N. Dey, Biogenic Polymer-Based Fluorescent Assemblies: Versatile Platforms for Ultrasensitive ATP Detection and Enzyme Assay, *Langmuir*, 2024, **40**(12), 6163–6171.
27 A. Pal and N. Dey, Surfactant-Induced Alterations in Optoelectronic Properties of Perylene Diimide Dyes: Modulating Sensing Responses in the Aqueous Environment, *Soft Matter*, 2024, **20**(14), 3044–3052.
28 A. Sharma, T. Gadly, A. Gupta, A. Ballal, S. K. Ghosh and M. Kumbhakar, Origin of Excitation Dependent Fluorescence in Carbon Nanodots, *J. Phys. Chem. Lett.*, 2016, **7**(18), 3695–3702.
29 H. V. Barkale and N. Dey, Membrane-Bound Bisindolyl-Based Chromogenic Probes: Analysis of Cyanogenic Glycosides in Agricultural Crops for Possible Remediation, *ACS Appl. Bio Mater.*, 2024, **8**(1), 189–198.
30 L. Satish, S. Millan and H. Sahoo, Spectroscopic Insight into the Interaction of Bovine Serum Albumin with Imidazolium-Based Ionic Liquids in Aqueous Solution, *Luminescence*, 2017, **32**(5), 695–705.
31 A. AYadav, S. Trivedi, V. Haridas, J. B. Essner, G. A. Baker and S. Pandey, Effect of Ionic Liquid on the Fluorescence of an Intramolecular Exciplex Forming Probe, *Photochem. Photobiol. Sci.*, 2020, **19**(2), 251–260.
32 B. Yadav, N. Yadav and P. Venkatesu, Unravelling the Stabilization Mechanism of Mono-, Di- and Tri-Cholinium Citrate–Ethylene Glycol DESs Towards α-Chymotrypsin for Preservation and Activation of the Enzyme, *Phys. Chem. Chem. Phys.*, 2024, **26**(44), 28025–28036.
33 A. Kumar, A. Rani and P. A. Venkatesu, Comparative Study of the Effects of the Hofmeister Series Anions of the Ionic Salts and Ionic Liquids on the Stability of α-Chymotrypsin, *New J. Chem.*, 2015, **39**(2), 938–952.
34 V. Sundaram, R. N. Ramanan, M. Selvaraj, N. Ahemad, R. Vijayaraghavan, D. R. MacFarlane and C. W. Ooi, Probing the Molecular Interactions between Cholinium-Based Ionic Liquids and Insulin Aspart: A Combined Computational and Experimental Study, *Int. J. Biol. Macromol.*, 2023, **253**, 126665.